Limnol. Oceanogr., 36(8), 1991, 1834–1850

Oceanic upwelling and productivity in the eastern tropical Pacific

Paul C. Fiedler and Valerie Philbrick
NOAA/NMFS Southwest Fisheries Science Center, P.O. Box 271, La Jolla, California 92038

Francisco P. Chavez
Monterey Bay Aquarium Research Institute, 160 Central Ave., Pacific Grove, California 93950

Abstract

An oceanographic survey of the eastern tropical Pacific Ocean in August–November 1990 found a productive, nutrient-rich, moderately high-chlorophyll surface layer in two oceanic upwelling regions: the equatorial divergence, especially east of the Galapagos, and the countercurrent divergence out to 105°W, >1,000 km west of the Costa Rica Dome. Although NO_3 is not depleted in upwelling regions, relationships among nutrient concentrations and temperature in 1986–1988 data from the same area show that NO_3 is the the first macronutrient to be depleted in adjacent, less-productive regions. A three-dimensional, two-layer box model of NO_3 flux within and into the euphotic zone gives estimated rates of new production that are ~29% of measured rates of ^{14}C phytoplankton production. Persistence of excess (saturating) NO_3 in the euphotic zone exceeds 1 yr under high-nutrient, low-chlorophyll conditions off the equator where weak upwelling, or downwelling, occurs. These results indicate substantial control or limitation of NO_3 utilization and productivity in nutrient-rich oceanic regions of the eastern tropical Pacific.

The eastern tropical Pacific contains some of the most productive waters of the world ocean. Concern about atmospheric CO_2 increase and the role of the deep ocean as a sink in the global C cycle has presented oceanographers with an important question: what are the rates of new production in large, productive areas of the open ocean and what limits those rates? Nutrients are rarely depleted in surface waters of the equatorial Pacific (Thomas 1979) or in other upwelling regions such as the Costa Rica Dome and coastal Peru and Ecuador. The thermocline is shallow in these regions, so that vertical advection and mixing bring cold, nutrient-rich water from below the thermocline (nutricline) into the surface layer. This nutrient input maintains optimal (saturating) concentrations of NO_3 at the surface and results in relatively high levels of new production (Chavez and Barber 1987), but not high enough to deplete NO_3. Persistence of nutrients at the sea surface characterizes the high-nutrient, low-chlorophyll (HNLC) condition that is the subject of this symposium (*see* Cullen 1991).

Surface currents and water masses of the eastern tropical Pacific are illustrated schematically in Fig. 1. Both coastal upwelling along eastern boundaries and oceanic upwelling along offshore divergences occur in this region. The effects of equatorial upwelling are evident in the equatorial thermocline ridge (Fig. 2) and in the anomalously cool temperature of equatorial surface water. Sverdrup et al. (1942) presented evidence of surface divergence and upwelling at two sites in the equatorial current system: in the South Equatorial Current along the equator, and between the North Equatorial Countercurrent and North Equatorial Current at 10°N. The countercurrent thermocline ridge along 10°N is evidence of upwelling in this countercurrent divergence. However, generally warm temperatures and low concentrations of nutrients suggest that the effects of upwelling do not reach the surface except at the eastern end of the ridge in the Costa Rica Dome. Offshore transport of surface waters and coastal upwelling are driven by equatorward. longshore winds along the coasts of Baja California and Peru-Ecuador and by topographically induced offshore winds at several points along the

Acknowledgments

We thank Stephen Reilly for continued support of this work, and the officers and crew of NOAA Ships *McArthur* and *David Starr Jordan*. John Cullen, David Behringer, and two reviewers provided critical comments.

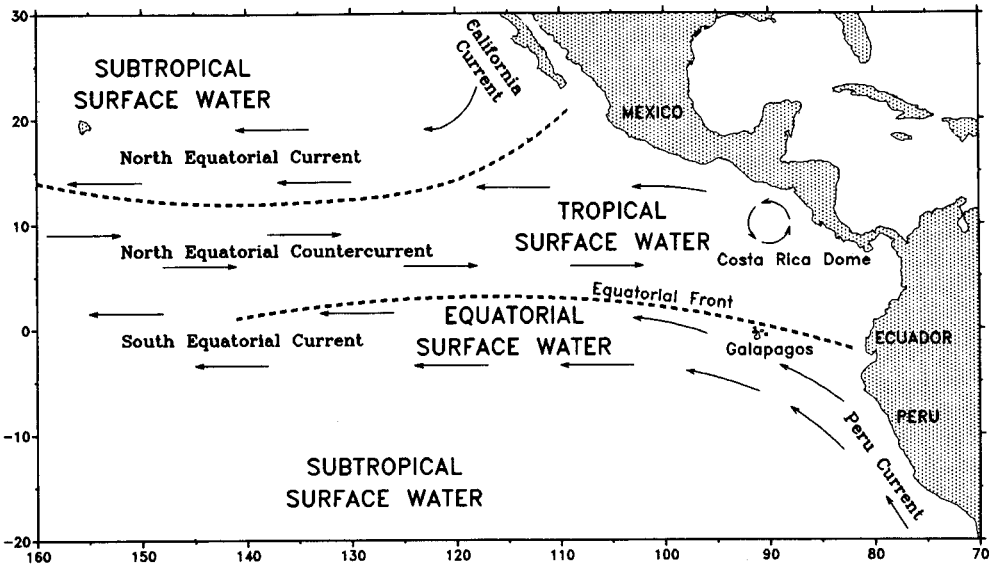

Fig. 1. Schematic diagram of eastern tropical Pacific surface water masses and surface currents (described by Wyrtki 1967).

coast of Central America (Gulfs of Tehuantepec, Papagayo, and Panama).

Chl and nutrient data have been collected in August–November in the eastern tropical Pacific since 1986 (Fiedler et al. 1992). These data, plus phytoplankton productivity measurements made in 1990, provide an opportunity to examine spatial patterns of nutrient availability and productivity. We examine PO_4-NO_3, SiO_4-NO_3, and NO_3-

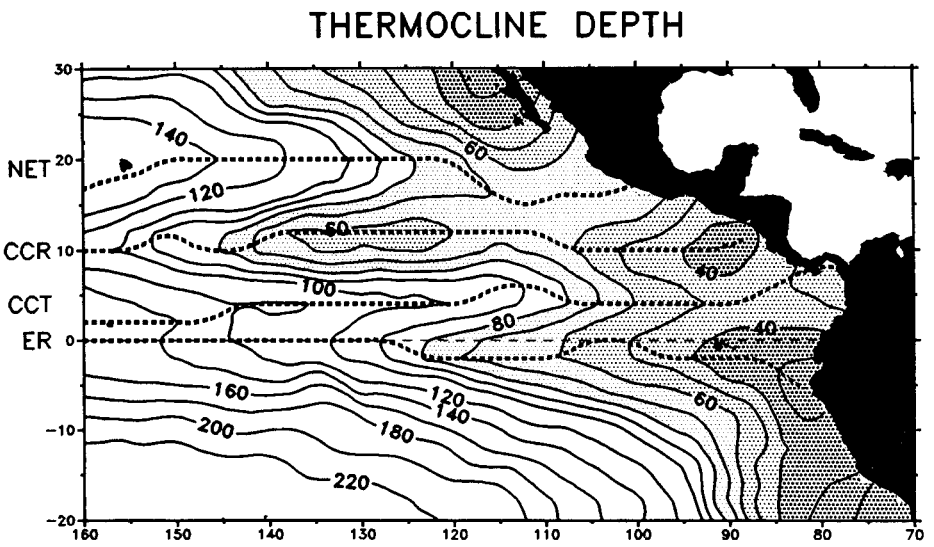

Fig. 2. August–November climatology of thermocline (20°C isotherm) depth (Fiedler 1992). ER—Equatorial ridge; CCT—countercurrent trough; CCR—countercurrent ridge; NET—north equatorial trough.

temperature relationships in our large data set to confirm that NO_3 depletion could limit productivity in parts of this region.

Surface current velocities calculated from ship drift reports were used to estimate horizontal transport and divergence within, and upwelling into, the mixed layer. From these rates and our observed NO_3 profiles, we calculated NO_3 fluxes into the euphotic zone and estimated rates of net NO_3 input (new production). New production is thus equal to the rate of NO_3 uptake necessary to maintain the observed NO_3 distribution in a steady state. Past estimates of production based on NO_3 input into the surface layer have used one-dimensional models and ignored horizontal loss or input of unused NO_3 in the euphotic zone (Riley 1956; Sapozhnikov and Galerkin 1973; Chavez and Barber 1987; Jenkins 1988; Yentsch 1990). In contrast, Roemmich (1989) performed a very thorough analysis of mass, heat, and salt balance in the Southern California Bight to derive an estimate of new production from net NO_3 import. Sarmiento et al. (1990) presented a model that estimates new production in the North Atlantic from horizontal and vertical NO_3 balances.

Methods

Field measurements—We collected oceanographic data in a large area of the eastern tropical Pacific (14×10^6 km^2) in August–November of 1986 through 1990. This sampling is part of a National Marine Fisheries Service program to monitor trends in relative abundance of dolphin stocks affected by the yellowfin tuna purse seine fishery. Sampling is constrained by daylight dolphin census operations. We collected XBT profiles, continuous records of surface temperature, salinity and (through 1989) fluorescence, and CTD casts with discrete samples for Chl and nutrient analysis and (in 1990 only) ^{14}C-uptake measurements.

Hydrocasts to 1,000 m were made 2 times per night with a Seabird or Neil-Brown CTD. General Oceanics Niskin bottles (1.7 liters) were retrofitted with silicon rubber O-rings in the valves and endcaps and silicon rubber tubing as the closing mechanism. The bottles were cleaned once a week by washing with a 25% MICRO cleaning solution, rinsing with freshwater, and soaking in 0.25 N HCl for 8 h. Ten rosette-mounted bottles collected water from eight standard depths (0, 20, 40, 60, 80, 100, 125, 150 m) plus two additional standard light depths for phytoplankton productivity casts as described below.

Ten 275-ml subsamples in the morning and eight samples in the evening were collected for phytoplankton pigment analysis. Samples were extracted for 24–36 h with 90% acetone in glass scintillation vials refrigerated in dark boxes. Chl *a* and pheophytin were measured with a Turner Designs model 10-005R fluorometer calibrated with commercial Chl *a* (Sigma). Subsamples (20 ml) were collected from morning productivity casts for nutrient analysis (NO_3, NO_2, PO_4, and SiO_4). These samples were frozen immediately after collection and analyzed later at Monterey Bay Aquarium Research Institute with an Alpkem autoanalyzer.

Water samples for determination of dissolved inorganic C uptake were collected from depths to which 100, 50, 30, 15, 5, 1, and 0.1% of the incident light penetrated. Light depths were estimated from expected euphotic zone depths calculated from pigment profiles observed on previous ETP dolphin surveys (1986–1989) according to Morel (1988). Samples were drawn into aged, "Vitro" glass 150-ml bottles (Wheaton Corp.) rinsed twice with sample water; 10 μCi of $NaH^{14}CO_3$ were added to each sample bottle and the bottles incubated in nickel screens (Perforated Products) in an on-deck seawater-cooled Plexiglas incubator for 24 h with natural sunlight as the light source. The screens act as neutral density filters, reducing the light intensity to the same level as at the depth from which the sample was collected. Two extra samples at the 100 and 0.1% light levels were inoculated with radioactive tracer and filtered immediately with no incubation to determine abiotic particulate ^{14}C incorporation (Chavez and Barber 1987).

For determination of particulate C fixation, the water was filtered onto Whatman GF/F filters at a vacuum of <5.2 cm of Hg, acidified with 0.5 N HCl, and counted in 10 ml of CytoScint ES on a liquid scintil-

lation counter after the 4-month cruise. Total ^{14}C activity was determined by adding 1.0 ml of incubated sample water (from the 100 and 30% light level bottles) to a scintillation vial containing 20 ml of Cytoscint ES cocktail. An average of these two values was used as the total amount of added inorganic C activity in the calculation of C uptake at a station.

Chl and pheopigment profiles measured at 20–25 m intervals were smoothed by cubic spline interpolation. The depth of the Chl maximum was determined from the smoothed Chl profile. Euphotic zone depth (Z_e, 1% PAR level) was calculated from Morel's relationship between Z_e and phytoplankton pigment concentration in the euphotic zone of oceanic case 1 waters, in which phytoplankton play a predominant role in determining optical properties (Morel 1988).

Box model of new production—A two-layer box model was used to calculate NO_3 fluxes into and within the surface layer. The model calculates new production as *the rate of NO_3 uptake necessary to maintain the observed NO_3 distribution in a steady state, given the climatological rates of vertical and horizontal advection derived from ship drift observations.* This new production maintains the steady state NO_3 distribution by loss of organic N from the euphotic zone (export production). Horizontal resolution was 2° × 2° latitude-longitude. The nutrient observations and ship drift data are not dense enough to resolve finer scale variability. New production in a 2° × 2° box was estimated as the net input of NO_3 into the surface layer (euphotic zone) by horizontal and vertical advection. Turbulent mixing from below and secondary sources such as terrestrial runoff and N_2 fixation were not considered, so that the estimates are valid only in upwelling areas and are probably underestimates even there. The model also excludes island effects and topographically induced upwelling that are not resolved by the 2° × 2° grid.

Mean [NO_3] in the euphotic zone (N_e) and [NO_3] at the base of the euphotic zone (N_z) were calculated from our 1986–1988 nutrient data. Euphotic zone depth for each cast was calculated from the phytoplankton pigment profile as described above. The nominal concentration at which uptake of NO_3 by oceanic phytoplankton approaches saturation is taken to be 4 μM (MacIsaac and Dugdale 1969). Thus, excess NO_3 ($N_e - 4.0 > 0$) occurs in the euphotic zone of nutrient-rich waters.

Surface currents were estimated from ship drift data in the National Oceanographic Data Center (NODC) surface current data set. A total of 35,205 ship drift reports in the study area from August to November (1900–1969) were averaged on a 2° × 2°-latitude-longitude grid. Observations were zonally smoothed during gridding by averaging observations within ±2° to 10° longitude of each grid point, so that at least 100 observations are included in each grid mean Fiedler 1992). This procedure ensured sample sizes adequate for estimation of a reliable mean at each grid point, while retaining resolution of the predominantly zonal structure of equatorial surface currents. Mean August–November surface-current vectors are plotted in Fig. 3, which also illustrates the 2° × 2° resolution of the box model.

Mixed-layer depth was estimated as the depth at which temperature is 0.5°C less than surface temperature in 24,928 XBT and MBT profiles collected in the study region in August–November from 1960 through 1989 (Fiedler 1992). The mixed layer defined in this way deepens from east to west and is deeper beneath the equatorial divergence than beneath the countercurrent divergence along 10°N (Fig. 3). This pattern has been observed in other analyses of mixed-layer depth in the eastern tropical Pacific (Wyrtki 1964; Levitus 1982).

Horizontal transports were calculated by assuming that the mean surface currents between boxes, derived from the ship drift data, were uniform through the mixed layer. Vertical transport through the base of the mixed layer was calculated from divergence of the horizontal transports. NO_3 flux was calculated from the product of transport and [NO_3] within or at the base of the euphotic zone. Thus, we assume that the vertical transport calculated at the base of the mixed layer can be applied to the base of the euphotic zone. Euphotic zone depth is 0–30

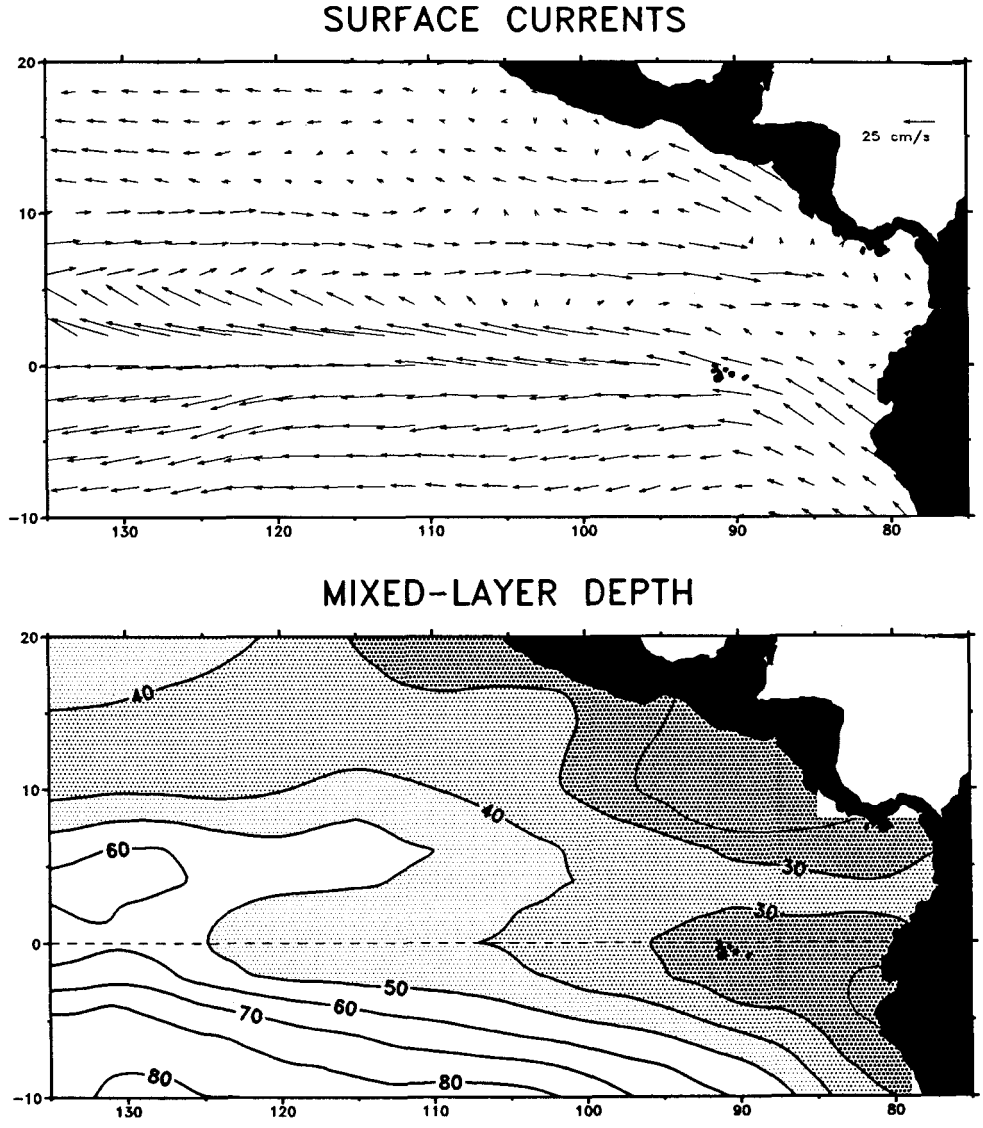

Fig. 3. Climatological August–November surface currents from ship drift data and mixed-layer depth (m) from XBT and MBT profiles.

m deeper than mixed-layer depth, except in the southwestern corner of the study area where the mixed layer is very deep.

Horizontal nutrient fluxes between boxes in the surface layer were calculated as the product of surface-current velocity, mean euphotic zone concentration, and mixed-layer depth times the length of the box edge (area of box side). A vertical flux into the surface layer (upwelling) was calculated as the product of net surface transport (out of a box) and nutrient concentration at the base of the euphotic zone. A vertical flux out of the surface layer (downwelling) was calculated as the product of net surface transport (into a box) and nutrient concentration in

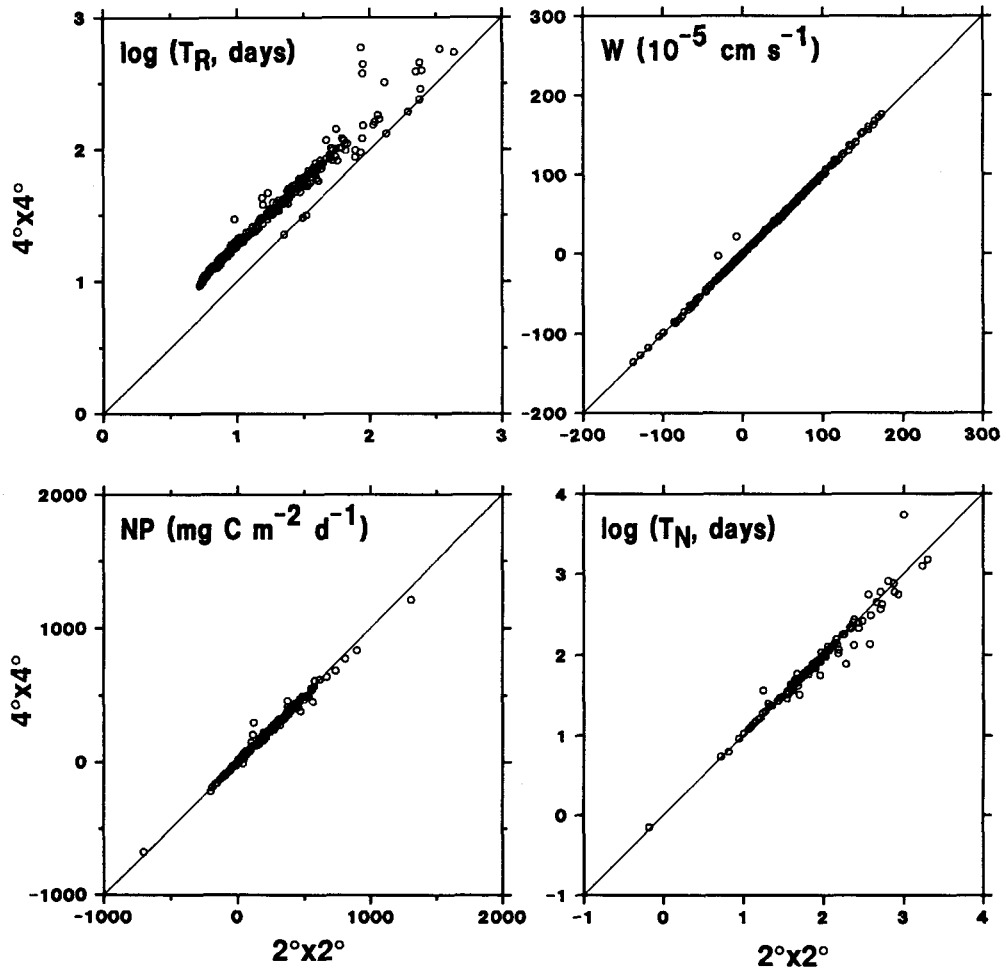

Fig. 4. Residence time (T_R), upwelling (W), new production (NP), and excess NO_3 persistence time (T_N) calculated at 2° × 2° and 4° × 4° resolution at model grid points.

the euphotic zone. Net NO_3 fluxes into the euphotic zone were converted to C production by the factor of 79.5 mg C (mmol N)$^{-1}$ [=106/16 mmol C (mmol N)$^{-1}$ × 12 mg C (mmol C)$^{-1}$]. This flux is equivalent to new production (NP, mg C m^{-2} d^{-1}).

An index of the persistence of excess NO_3 in the euphotic zone was calculated as the excess NO_3 content of the euphotic zone [$Z_e(N_e - 4.0)$, mmol N m^{-2}] divided by net NO_3 input (mmol N m^{-2} d^{-1}). Excess NO_3 persistence time (T_N, d) represents the time required for phytoplankton uptake to deplete the excess NO_3 if NO_3 flux into the euphotic zone ceases. T_N is comparable to turnover times calculated from measured nutrient uptake rates and concentrations in the mixed layer or euphotic zone, although turnover times refer to uptake of the total, not excess, nutrient content.

Residence time of water within a box was calculated as the box volume divided by the total rate of inflow (or outflow). The effect of residence time of water in a box on rates estimated by the model was tested by comparing model results at 2° × 2° and 4° × 4° resolution. Residence time, rates of upwelling and new production, and excess NO_3

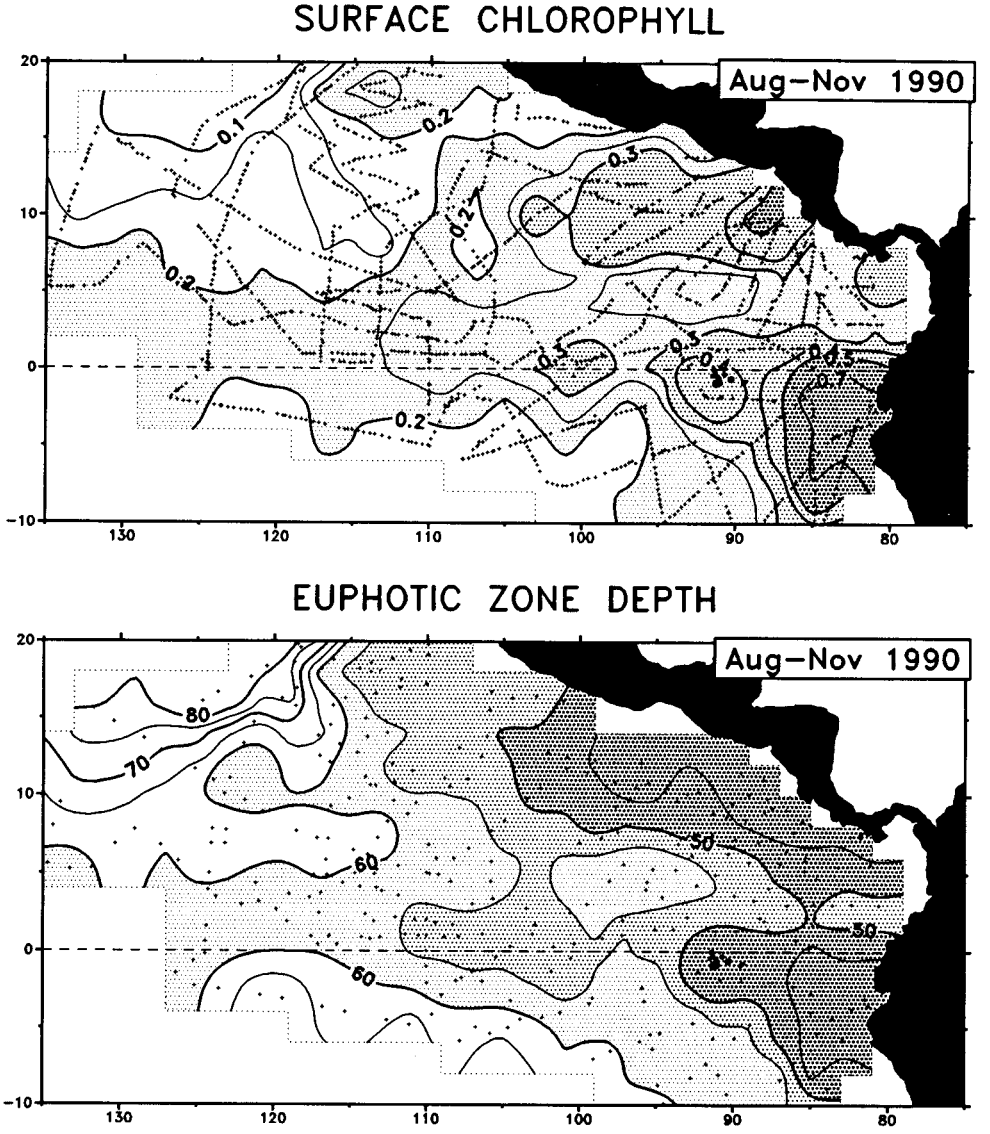

Fig. 5. Surface Chl concentration (mg m^{-3}) and euphotic zone depth (m), August–November 1990.

persistence time were calculated for the same grid points at each resolution. The results show that, although residence time increases by a factor of ~2 when box size is doubled, the other rates do not change (Fig. 4). The few points that do not fall along the 1 : 1 line represent boxes at the edges of the model domain where 4° × 4° boxes do not resolve the boundary as well as 2° × 2° boxes. Thus, rates derived from the model are not directly affected by model resolution and its effect on residence time.

Results

Observations—In August–November 1990, surface Chl was high (>0.2 mg m^{-3}) along both the equatorial and countercurrent divergences (Fig. 5). Values were high-

est (>0.4 mg m^{-3}) off the coast of Ecuador, around the Galapagos Islands, and at the Costa Rica Dome. The euphotic zone deepened from <45 m off Ecuador and Central America to >80 m in oligotrophic subtropical waters in the NW corner of the study area. Mean euphotic zone Chl (not shown, but directly related to Z_e by definition) showed the same basic pattern as surface Chl, except that relatively high values extended out beyond 110°W along the countercurrent divergence. Z_e was strongly correlated with the depth of the Chl maximum (Fig. 6, $r = 0.77$). In general, the Chl_{max} occurred below the 1% light level where Z_e > 60 m, toward the oligotrophic subtropical surface water masses of the North and South Pacific.

Phytoplankton productivity (PP) and productivity index ($PI = \int_z PP / \int_z$ Chl) were high [>600 mg C m^{-2} d^{-1} and >40 mg C (mg Chl)$^{-1}$ d^{-1}] along both the equatorial and countercurrent divergences out to 100°–110°W (Fig. 7). Along the countercurrent divergence, productivity was higher to the west of the Costa Rica Dome than in the dome itself (the surface Chl_{max} at 10°N, 88°W). A band of moderately high productivity extended west of 110°W along the equator.

NO_3 was depleted before SiO_4 or PO_4 in the 1986–1988 samples (Fig. 8, Table 1). The positive intercepts of the linear regressions of SiO_4 and PO_4 on NO_3 are 1.48 μM SiO_4 and 0.28 μM PO_4, both significantly different from zero ($P < 0.001$). The reciprocal of the slope of the PO_4-NO_3 regression is 16.1, compared to the N : P Redfield ratio of 16 : 1 (Redfield 1958). NO_3 decreases as water temperature increases (Fig. 9, Table 1). The regression line passes through 4 μM NO_3 at 25.4°C.

Nutrient-rich (>4 μM NO_3) surface waters were observed south of 2°N in 1986–1988 (Fig. 10). These correspond approximately to the equatorial and Peru Current surface-water masses described by Wyrtki (1967), although the nutrient-rich oceanic surface waters are not symmetric about the equator (*see also* Thomas 1979). The distribution of mean euphotic zone [NO_3] (N_e) indicates that nutrient-rich water is found deeper in the euphotic zone in tropical surface water north of the equatorial surface water and east of 105°W. [NO_3] at the bottom of the euphotic zone is as high or higher along the countercurrent divergence as along the equator.

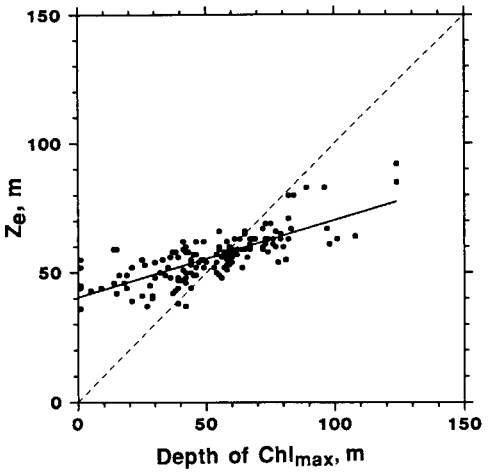

Fig. 6. Relationship between Z_e (m) and depth of the Chl_{max} (m), August–November 1990.

Phytoplankton productivity observed in 1990 was significantly correlated with euphotic zone NO_3 (N_e, Fig. 11, $r = 0.47$). The significance of the Pearson correlation coefficient ($P < 0.0001$) was confirmed by a nonparametric test (Kendall's τ, Conover 1971). Normalizing productivity to Chl weakens the relationship slightly ($r = 0.42$), because N_e is related to euphotic zone pigment content through the derivation of Z_e.

Model—Divergence of surface currents results in strong upwelling along the equator, especially west of 115°W (Fig. 12). Weaker upwelling occurs along the countercurrent divergence at the coast and between 95° and 100°W, and in the northwest corner of the study area at the edge of the North Pacific subtropical gyre. The upwelling rates derived from ship drift data along the equatorial and countercurrent divergences are consistent with rates estimated by other methods (Fiedler 1992).

Estimated new production is positive in upwelling areas and in adjacent areas where unused NO_3 is advected horizontally from upwelling areas (Fig. 13). Highest rates occur in the equatorial divergence and in the

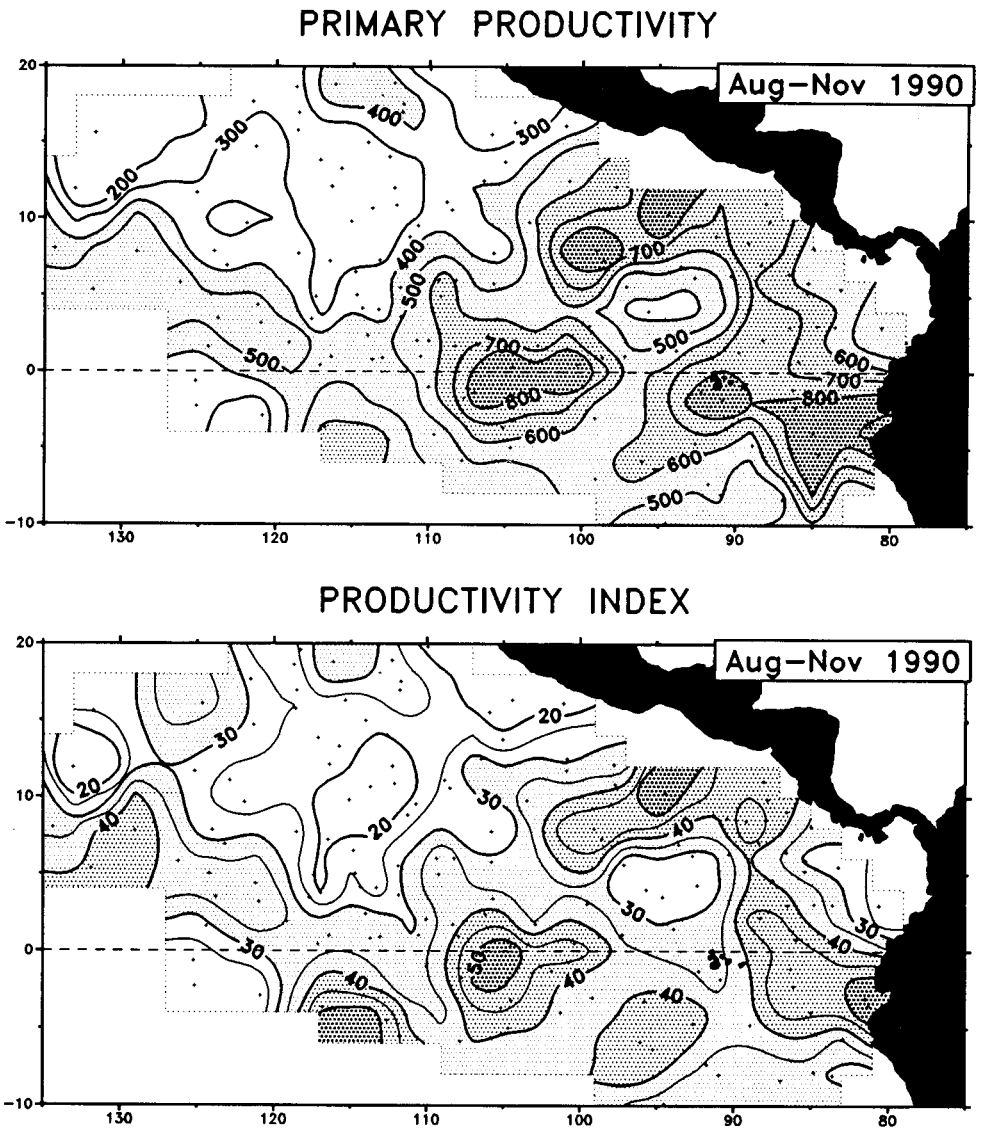

Fig. 7. Phytoplankton productivity (mg C m^{-2} d^{-1}) and productivity index [mg C (mg Chl)$^{-1}$ d^{-1}], August–November 1990.

countercurrent divergence near the Costa Rica Dome. Estimated new production in upwelling areas ($W > 5 \times 10^{-5}$ cm s^{-1}) is significantly correlated with ^{14}C phytoplankton productivity measured in 1990 (Fig. 14, $r = 0.48$). The slope of the regression line is equivalent to an f-ratio (Eppley and Peterson 1979) and equals 0.29 (± 0.11, 95% C.L.). Log-transformation does not significantly improve the regression relationship ($r = 0.50$).

Persistence of excess NO_3 in the euphotic zone, estimated from the model for 2° × 2° boxes with a positive net input of NO_3 (new production), is illustrated in Fig. 15. NO_3 persistence varies from 0.4 to >1,000 d

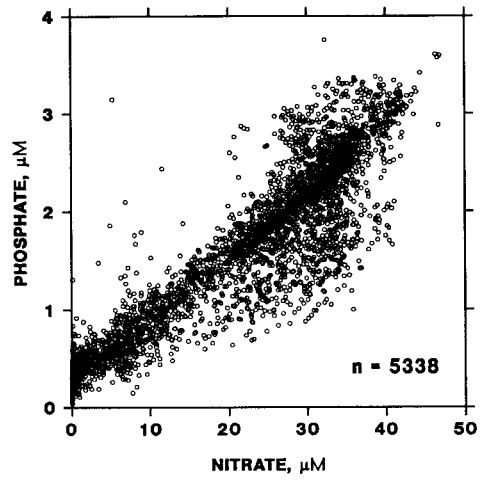

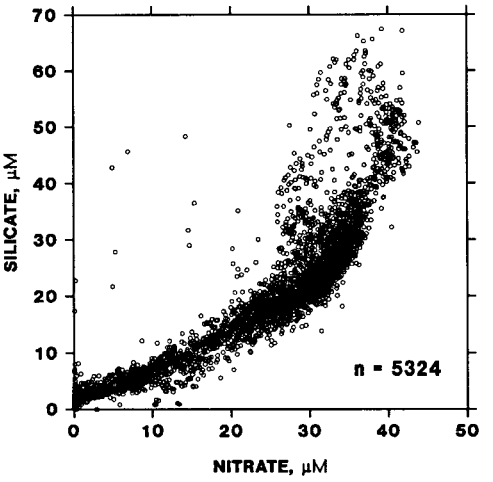

Fig. 8. PO_4-NO_3 and SiO_4-NO_3 relationships for the eastern tropical Pacific, August–November 1986–1988.

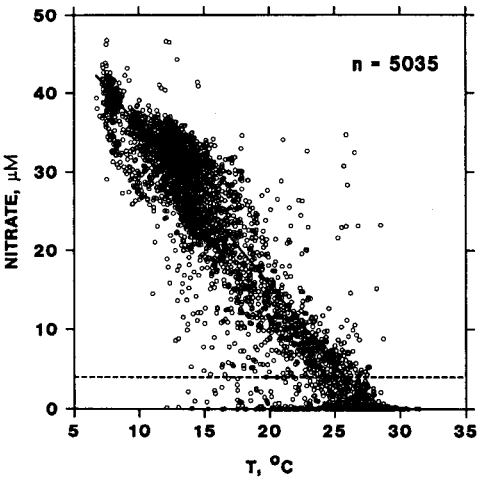

Fig. 9. NO_3-temperature relationship for the eastern tropical Pacific, August–November 1986–1988. Dashed line at 4 μM represents nominal concentration at which uptake by oceanic phytoplankton is saturated.

(median = 70). Persistence is shortest (<70 d) in the strong upwelling regions off Ecuador and along the northern edge of the equatorial divergence. Persistence is longest (>500 d) in tropical surface waters between the equatorial front and the coast of Central America, including waters at the Costa Rica Dome and along the countercurrent divergence.

Discussion

NO_3 can be depleted in the eastern tropical Pacific, but generally only in waters warmer than 25°C. Equatorial surface water rarely exceeds this temperature in August–November, except during El Niño. Tropical surface water is warmer than 27°C, even above the shallow thermocline in the countercurrent divergence at the eastern end of the countercurrent thermocline ridge (including the Costa Rica Dome). Euphotic zone waters are nutrient-rich (>4 μM N) along the equator and in tropical surface water north of 4°N and east of 105°W. We observed high phytoplankton biomass and productivity in these regions, especially in the two oceanic upwelling regions extending

Table 1. Nutrient and temperature relationships in the eastern tropical Pacific, August–November 1986–1988. All regressions are significant at $P < 0.001$.

$[SiO_4] = 0.635[NO_3] + 1.48$	$r = 0.89$	$n = 2{,}709$*
$[PO_4] = 0.062[NO_3] + 0.284$	$r = 0.94$	$n = 5{,}338$
$[NO_3] = -2.040T + 55.78$	$r = 0.95$	$n = 5{,}035$

* For $[NO_3] < 25$ μM.

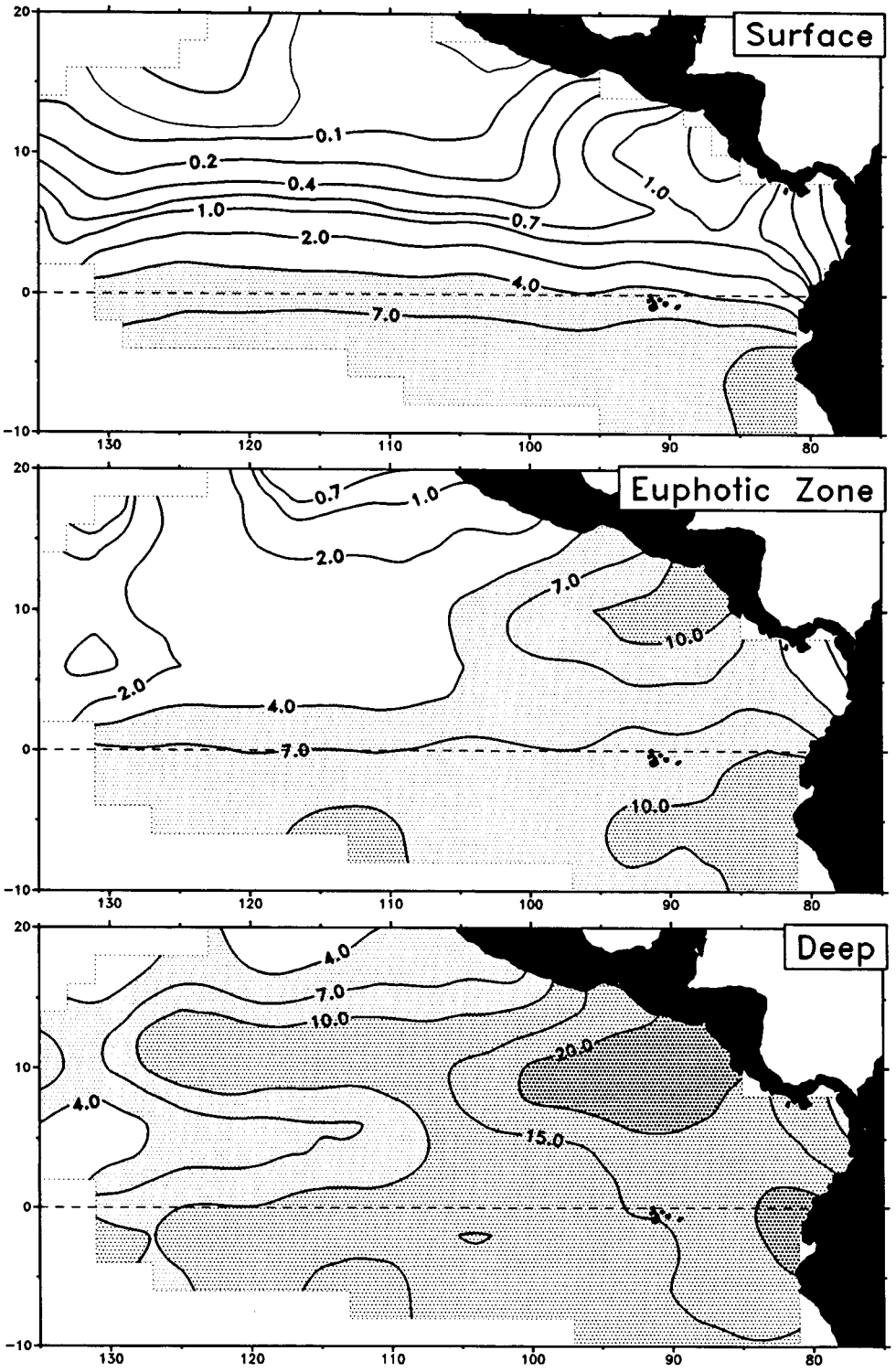

Fig. 10. $[NO_3]$ (μM) at the surface, averaged over the euphotic zone, and at the euphotic zone depth, August–November 1986–1988.

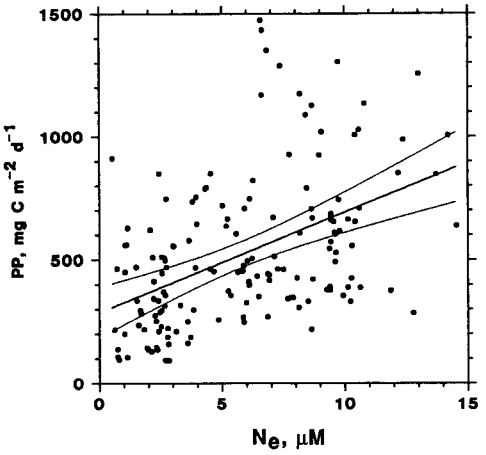

Fig. 11. Relationship between phytoplankton productivity (*PP*, mg C m^{-2} d^{-1}), August–November 1990, and 1986–1988 euphotic zone NO_3 (N_e, μM).

zonally to 105°W from the coast of Ecuador and the Costa Rica Dome.

Our measured rates of ^{14}C phytoplankton productivity are within the range reported by others using techniques to reduce trace metal contamination. We observed rates of 400–800 mg C m^{-2} d^{-1} in equatorial water between the Galapagos and 140°W. Rates observed previously in this region range between 400 and 1,000 (Chavez and Barber 1987; Chavez 1989; Chavez et al. 1990). Berger (1989), in a comprehensive global compilation of ^{14}C phytoplankton productivity rates (including measurements that may be biased by trace metal contamination), showed a range of 300–500 (up to 1,500 in a few small areas) in the eastern equatorial Pacific and in tropical waters east of 105°W. We observed rates of 200–400 mg C m^{-2} d^{-1} in tropical surface water west of 105°W. These values are comparable to other reported rates in this region: 200–500 at four stations along 110°W between 3° and 9°N (Chavez et al. 1990) and 100–200 along 126°W and 138°W (El-Sayed and Taguchi 1979). Berger (1989) showed a range of 100–300 in this region. EASTROPAC is the only other survey to have measured phytoplankton productivity in the eastern tropical Pacific over an area nearly as large as we did (Owen and Zeitzschel 1970). However, the EASTROPAC rates are much lower than more recent estimates, due to unresolved methodological problems (Banse and Yong 1990).

We observed productivity indices of 30–50 mg C (mg Chl)$^{-1}$ d^{-1} in equatorial and countercurrent divergence upwelling regions. Barber and Chavez (1991) reported areal means of 30.4–46.6 in the eastern equatorial Pacific between 84° and 140°W; Voiturez and Herbland (1977) reported "typical tropical" Atlantic values of 22–58. Mean productivity indices reported for coastal upwelling regions are in the same

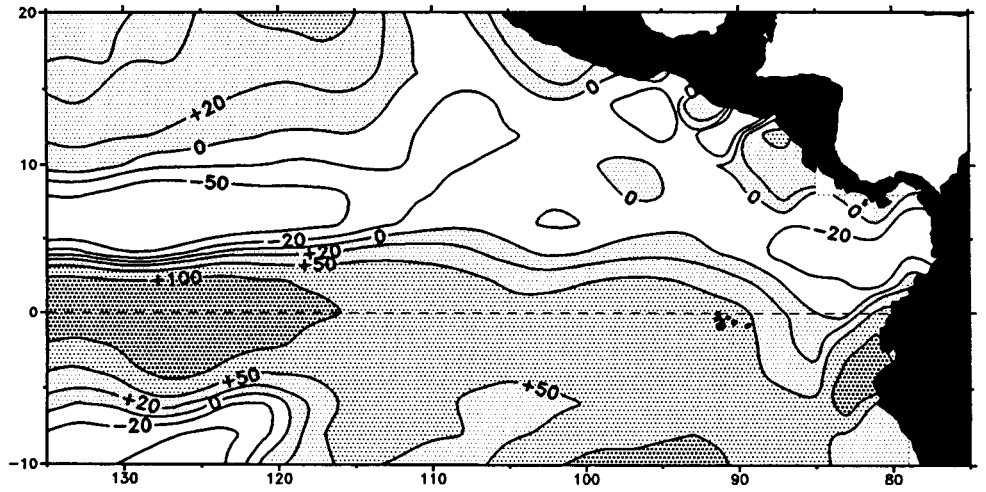

Fig. 12. August–November climatology of upwelling velocity (10^{-5} cm s^{-1}) at the base of the mixed layer derived from surface current divergence.

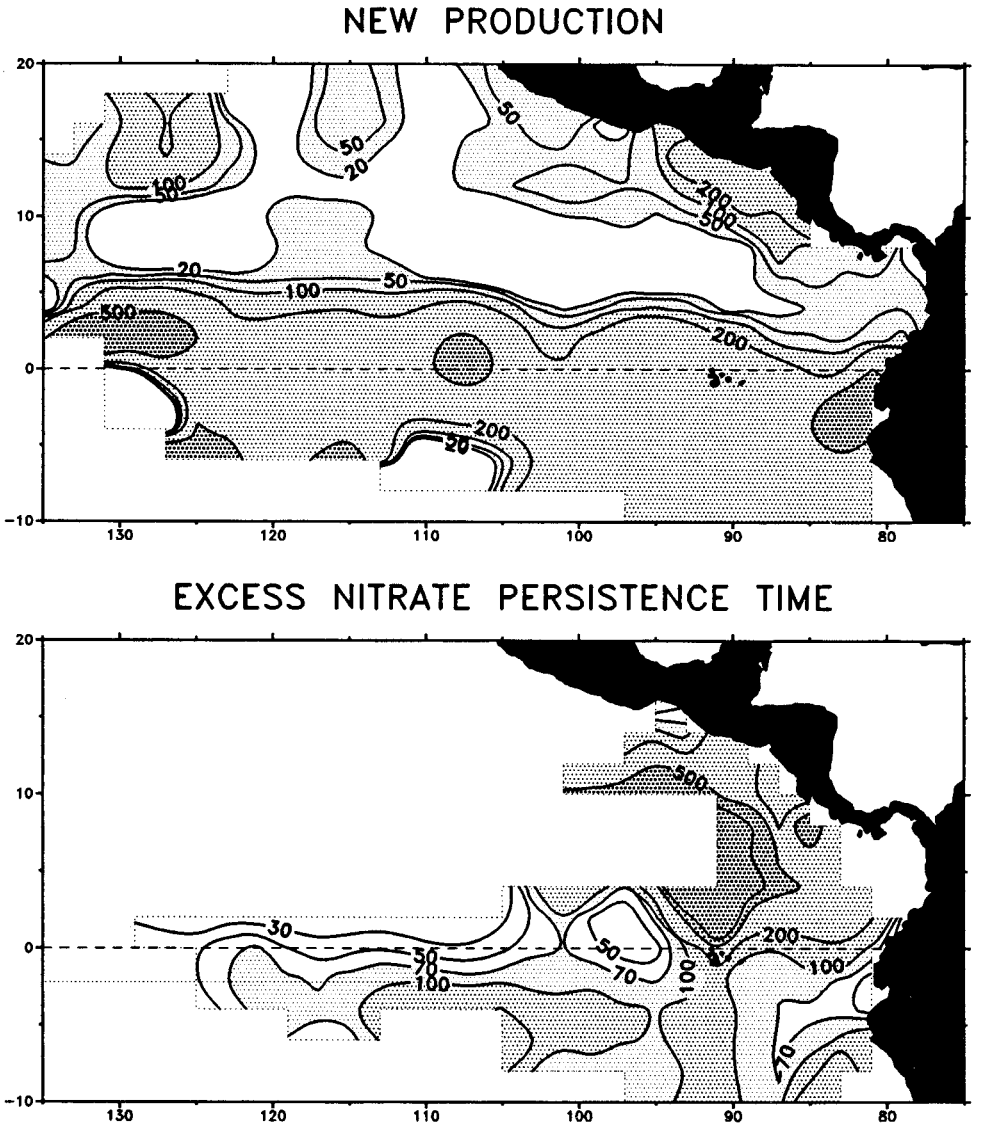

Fig. 13. New production (mg C m^{-2} d^{-1}) and persistence of excess NO_3 (>4 μM) in the euphotic zone (d), estimated from the box model of NO_3 advective flux and uptake in the eastern tropical Pacific.

range: Peru—39 and 47 (Chavez and Barber 1987; Barber and Smith 1981); Northwest Africa—34 (Barber and Smith 1981); California Current—33 (Hayward and Venrick 1982). Lower productivity indices have been reported for other regions: 2–27 in the nutrient-limited North Pacific subtropical gyre and Sargasso Sea (Sharp et al. 1980; Prézelin and Glover 1991); 2–10 in the light-limited Southern Ocean (El-Sayed and Turner 1977; Holm-Hansen et al. 1977); 18.5 in the Southern California Bight (Eppley et al. 1985); and 8–22 in the subarctic Pacific (McAllister et al. 1960).

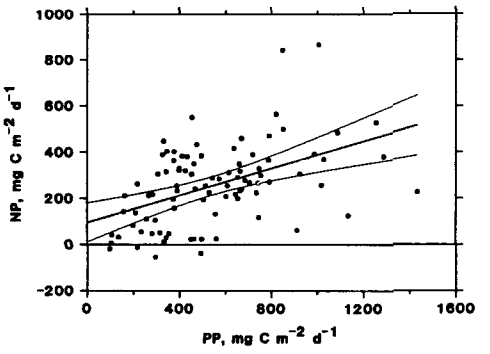

Fig. 14. Estimated new production (*NP*, mg C m^{-2} d^{-1}) vs. measured ^{14}C phytoplankton productivity (*PP*, mg C m^{-2} d^{-1}) at stations in climatological upwelling regions ($W > 5 \times 10^{-5}$ cm s^{-1}) of the eastern tropical Pacific, August–November 1990 ($n = 92$). Linear regression ±95% C.L.: $NP = 0.293PP + 95.4$, $r = 0.48$, $P < 0.00001$.

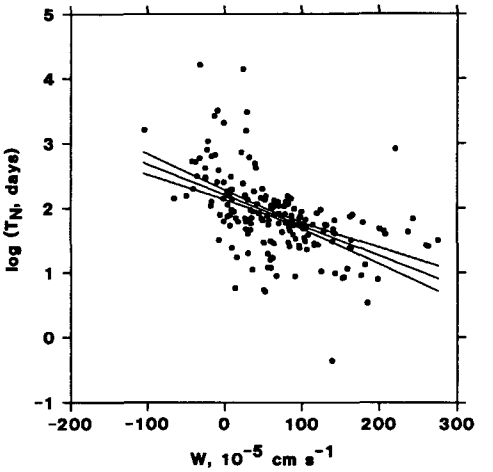

Fig. 15. Relationship between excess NO_3 persistence time (T_N, d) and upwelling rate (W, 10^{-5} cm s^{-1}) in the box model of NO_3 advective flux and uptake in the eastern tropical Pacific. Solid lines represent linear regression ±95% C.L.

The apparent equatorial minimum at the Galapagos in the map of productivity index (Fig. 7) is defined by two stations ~100 km south of the islands. Barber and Chavez (1991), however, observed a relatively high mean productivity index at 19 stations in the Galapagos region, mostly along 92°W (50 km west of the islands) between 5°N and 5°S. Although the phytoplankton community in the equatorial Pacific is generally dominated by several small, solitary phytoplankton groups, relatively high diatom abundances have been observed near the Galapagos (Jimenez 1981). Differences in species composition between these two sites, especially in the relative abundance of diatoms, could affect the C : Chl ratio (Geider 1987), resulting in differences in productivity per unit Chl.

Although we do not have nutrient measurements available for our 1990 productivity stations, integrated phytoplankton productivity in the euphotic zone was significantly correlated with the NO_3 field observed in 1986–1988. This relationship suggests nutrient limitation of productivity in the nutrient-poor tropical and subtropical surface waters west of 105°W and north of 5°N in the eastern tropical Pacific. The strength of the relationship between productivity and [NO_3] does not increase when productivity is normalized to Chl.

Empirical and theoretical relationships between phytoplankton productivity per unit sea surface normalized to Chl (productivity index) and solar insolation have been explored by Platt et al. (1988) and Cullen (1990). General growth models reviewed by Cullen (1990) predict a *PI* of ~40 mg C (mg Chl)$^{-1}$ d^{-1} for a typical summer insolation in the eastern equatorial Pacific (70 Einst m^{-2} d^{-1}). *PI* is independent of nutrient limitation in such models and cannot be used to infer effects of nutrients on specific growth rates.

Our model indicates high rates of new production in the upwelling regions along the equator and at the Costa Rica Dome. New production also occurs in some downwelling areas, such as between the equatorial and countercurrent divergences east of 90°W and along the coast of Mexico to the northwest of the Costa Rica Dome. This production is driven by horizontal advection of unused NO_3 from adjacent upwelling areas.

Estimated new production based on climatological surface currents and 1986–1988 NO_3 distribution is significantly correlated with measured 1990 phytoplankton productivity. The relationship would presum-

ably be stronger if we were able to use 1990 surface current and nutrient data to estimate new production. The slope of the regression line is 0.29 (±0.11), representing an average *f*-ratio (new/total production). Eppley and Peterson (1979) estimated *f*-ratios of 0.13–0.30 for the water types found in the eastern tropical Pacific (transitional, equatorial divergence, and inshore waters), and Dugdale (1976) reported measured *f*-ratios of 0.17–0.21. Eppley and Peterson (1979) found that the *f*-ratio increases with total productivity, but the scatter in our results is too great to resolve a nonlinear relationship.

The major discrepancy between the estimated and measured rates is the difference in zonal gradients of productivity. Measured rates of phytoplankton productivity decline to the west along both the countercurrent and equatorial divergences. In contrast, the model estimates relatively high rates of upwelling and new production along the equator west of the Galapagos and at the edge of the subtropical gyre. This difference may indicate that the model's direct relationship between transports and mixed-layer depth, which increases from east to west, is inadequate to describe the advective regime.

The extent of HNLC conditions in the eastern tropical Pacific is delimited by the region of excess NO_3 persistence in Fig. 13 (cf. Figs. 5 and 10). Excess NO_3 persistence time (T_N) is an index of limitation or control of NO_3 uptake (new production). T_N is inversely correlated with upwelling rate (W, Fig. 15, $r = -0.52$). This result is partially a consequence of the definition of $T_N [= Z_e(N_e - 4)/N'$, where N' = net NO_3 input], because W is weakly correlated with $Z_e(N_e - 4)$ ($r = +0.14$) and positively correlated with N' ($r = +0.37$).

Turnover times of euphotic zone N in the oligotrophic North Pacific central gyre are 3–15 d (Eppley et al. 1973). Turnover times in coastal upwelling systems are also on the order of a few days (Zimmerman et al. 1987). In contrast, NO_3 uptake rates measured at the surface in the central equatorial Pacific (150°W) indicate a NO_3 turnover time of >120 d and a T_N of >35 d (Wilkerson and Dugdale 1992), which is consistent with the model estimates of excess NO_3 persistence along the equator. In weak upwelling and downwelling HNLC conditions in the eastern tropical Pacific, NO_3 persists for >100 d at concentrations that should saturate uptake by phytoplankton, which indicates limitation or control of uptake and new production by a factor other than NO_3. Alternative hypotheses include control of phytoplankton biomass by grazing and limitation of NO_3 uptake by Fe deficiency (Cullen 1991). Our observations and model results are not adequate for conclusive tests of these hypotheses.

Our survey of the eastern tropical Pacific confirmed moderately high rates of phytoplankton production in oceanic upwelling regions along the equatorial and countercurrent divergences. In nutrient-poor regions of the eastern tropical Pacific, productivity is apparently limited by NO_3 availability. A box model of NO_3 flux, based on observed surface currents and NO_3 distribution, indicates that rates of NO_3 utilization or new production in upwelling regions is much lower than the rate of input of upwelled NO_3 into the euphotic zone. Excess NO_3 persists in the euphotic zone and is advected to adjacent weak upwelling and downwelling regions, where it can persist for >200 d. Grazing, Fe deficiency, or other hypotheses of limitation of productivity must explain this long persistence of NO_3 in the well-lighted HNLC waters of the eastern tropical Pacific.

References

BANSE, K., AND M. YONG. 1990. Sources of variability in satellite-derived estimates of phytoplankton production in the eastern tropical Pacific. J. Geophys. Res. **95:** 7201–7215.

BARBER, R. T., AND F. P. CHAVEZ. 1991. Regulation of primary productivity rate in the equatorial Pacific. Limnol. Oceanogr. **36:** 1793–1802.

———, AND R. L. SMITH. 1981. Coastal upwelling ecosystems, p. 31–68. *In* A. R. Longhurst [ed.], Analysis of marine ecosystems. Academic.

BERGER, W. H. 1989. Appendix: Global maps of ocean productivity, p. 429–455. *In* W. H. Berger et al. [eds.], Productivity of the ocean: Present and past. Wiley.

CHAVEZ, F. P. 1989. Size distribution of phytoplankton in the central and eastern tropical Pacific. Global Biogeochem. Cycles **3:** 27–35.

———, AND R. T. BARBER. 1987. An estimate of new production in the equatorial Pacific. Deep-Sea Res. **34:** 1229–1243.

———, K. R. BUCK, AND R. T. BARBER. 1990. Phytoplankton taxa in relation to primary production in the equatorial Pacific. Deep-Sea Res. **37:** 1733–1752.

CONOVER, W. J. 1971. Practical nonparametric statistics. Wiley.

CULLEN, J. J. 1990. On models of growth and photosynthesis in phytoplankton. Deep-Sea Res. **37:** 667-683.

———. 1991. Hypotheses to explain high-nutrient conditions in the open sea. Limnol. Oceanogr. **36:** 1578–1599.

DUGDALE, R. C. 1976. Nutrient cycles, p. 141–172. *In* D. H. Cushing and J. J. Walsh [eds.], The ecology of the seas. Saunders.

EL-SAYED, S. Z., AND S. TAGUCHI. 1979. Phytoplankton standing crop and primary productivity in the tropical Pacific, p. 241–286. *In* J. L. Bischoff and D. Z. Piper [eds.], Marine geology and oceanography of the Pacific manganese nodule province. Plenum.

———, AND J. T. TURNER. 1977. Productivity of the Antarctic and subtropical regions: A comparative study, p. 463–504. *In* Polar oceans. Proc. SCOR/SCAR Conf.

EPPLEY, R. W., AND B. J. PETERSON. 1979. Particulate organic matter flux and planktonic new production in the deep ocean. Nature **282:** 677–680.

———, E. H. RENGER, E. L. VENRICK, AND M. M. MULLIN. 1973. A study of plankton dynamics and nutrient cycling in the central gyre of the north Pacific Ocean. Limnol. Oceanogr. **18:** 534–551.

———, E. STEWART, M. R. ABBOTT, AND U. HEYMAN. 1985. Estimating ocean production from satellite chlorophyll. Introduction to regional differences and statistics for the Southern California Bight. J. Plankton Res. **7:** 57–70.

FIEDLER, P. C. 1992. Seasonal climatologies and variability of eastern tropical Pacific surface waters. NOAA Tech. Rep. NMFS. In press.

———, F. P. CHAVEZ, D. W. BEHRINGER, AND S. B. REILLY. 1992. Physical and biological effects of Los Niños in the eastern tropical Pacific, 1986–1989. Deep-Sea Res. **39:** In press.

GEIDER, R. J. 1987. Light and temperature dependence of the carbon to chlorophyll *a* ratio in microalgae and cyanobacteria: Implications for physiology and growth of phytoplankton. New Phytol. **106:** 1–34.

HAYWARD, T. L., AND E. L. VENRICK. 1982. Relation between surface chlorophyll, integrated chlorophyll and primary production. Mar. Biol. **69:** 247–252.

HOLM-HANSEN, O., S. Z. EL-SAYED, G. A. FRANCESCHINI, AND R. L. CUHEL. 1977. Primary production and factors controlling phytoplankton growth in the Southern Ocean, p. 11–50. *In* G. A. Llano [ed.], Adaptations within the Antarctic ecosystems. Gulf.

JENKINS, W. J. 1988. Nitrate flux into the euphotic zone near Bermuda. Nature **331:** 521–523.

JIMENEZ, R. 1981. Composition and distribution of phytoplankton in the upwelling systems of the Galapagos Islands, p. 327–338. *In* F. A. Richards [ed.], Coastal upwelling. Coastal Estuarine Sci. V. 1. AGU.

LEVITUS, S. 1982. Climatological atlas of the world ocean. NOAA Prof. Pap. 13. U.S. GPO.

MCALLISTER, C. D., T. R. PARSONS, AND J. D. H. STRICKLAND. 1960. Primary productivity and fertility at Station "P" in the northeast Pacific Ocean. J. Cons. Cons. Int. Explor. Mer **25:** 240–259.

MACISAAC, J. J., AND R. C. DUGDALE. 1969. The kinetics of nitrate and ammonia uptake by natural populations of marine phytoplankton. Deep-Sea Res. **16:** 45–57.

MOREL, A. 1988. Optical modeling of the upper ocean in relation to its biogenous matter content (Case 1 waters). J. Geophys. Res. **93:** 10,749–10,768.

OWEN, R. W., AND B. ZEITZSCHEL. 1970. Phytoplankton production: Seasonal change in the oceanic eastern tropical North Pacific. Mar. Biol. **7:** 32–36.

PLATT, T., S. SATHYENDRANATH, C. M. CAVERHILL, AND M. R. LEWIS. 1988. Ocean primary production and available light: Further algorithms for remote sensing. Deep-Sea Res. **35:** 855–879.

PRÉZELIN, B. B., AND H. E. GLOVER. 1991. Variability in time/space estimates of phytoplankton, biomass and productivity in the Sargasso Sea. J. Plankton Res. **13**(suppl.): 45–67.

REDFIELD, A. C. 1958. The biological control of chemical factors in the environment. Am. Sci. **46:** 205–221.

RILEY, G. A. 1956. Oceanography of Long Island Sound, 1952–1954. 4. Production and utilization of organic matter. Bull. Bingham Oceanogr. Collect. **15:** 324–344.

ROEMMICH, D. 1989. Mean transport of mass, heat, salt and nutrients in southern California coastal waters: Implications for primary production and nutrient cycling. Deep-Sea Res. **36:** 1359–1378.

SAPOZHNIKOV, V. V., AND L. I. GALERKIN. 1973. Calculation of primary production in tropical waters from the upward influx of biogenic elements, p. 67–72. *In* M. E. Vinogradov [ed.], Life activity of pelagic communities in the ocean tropics. Israel Program Sci. Transl.

SARMIENTO, J. L., G. THIELE, R. M. KEY, AND W. S. MOORE. 1990. Oxygen and nitrate new production and remineralization in the North Atlantic subtropical gyre. J. Geophys. Res. **95:** 18,303–18,315.

SHARP, J. H., M. J. PERRY, E. H. RENGER, AND R. W. EPPLEY. 1980. Phytoplankton rate processes in the oligotrophic waters of the central North Pacific Ocean. J. Plankton Res. **2:** 335–353.

SVERDRUP, H. U., M. W. JOHNSON, AND R. H. FLEMING. 1942. The oceans. Prentice-Hall.

THOMAS, W. H. 1979. Anomalous nutrient chlorophyll interrelationships in the offshore eastern tropical Pacific Ocean. J. Mar. Res. **37:** 327–335.

VOITUREZ, B., AND A. HERBLAND. 1977. Étude de la production pélagique de la zone équatoriale de

l'Atlantique à 4°W. Cah. ORSTOM Ser. Oceanogr. **25:** 313–331.

WILKERSON, F. P., AND R. C. DUGDALE. 1992. Measurements of nitrogen productivity in the equatorial Pacific. J. Geophys. Res. **97:** 669–679.

WYRTKI, K. 1964. The thermal structure of the eastern Pacific Ocean. Dtsch. Hydrogr. Z. Suppl., p. 1–84.

———. 1967. Circulation and water masses in the eastern equatorial Pacific Ocean. Int. J. Oceanol. Limnol. **1:** 117–147.

YENTSCH, C. S. 1990. Estimates of "new production" in the mid-North Atlantic. J. Plankton Res. **12:** 717–734.

ZIMMERMAN, R. C., J. N. KREMER, AND R. C. DUGDALE. 1987. Acceleration of nutrient uptake by phytoplankton in a coastal upwelling ecosystem: A modeling analysis. Limnol. Oceanogr. **32:** 359–367.